Interaction of 8 MeV/μ Xe^{21+} with Carbon Foils

Laura Jeanne Cook

University Undergraduate Fellow, 1993-1994

Texas A&M University

Department of Physics

APPROVED

Fellows Advisor ____________________

Honors Director ____________________

Interaction of 8 MeV/μ Xe^{21+} with Carbon Foils

Laura Jeanne Cook

University Undergraduate Fellow, 1993-1994

Texas A&M University

Department of Physics

APPROVED

Fellows Advisor ____________________________

Honors Director ____________________________

Table of Contents

I. Introduction

The charge of an energetic ion passing through matter fluctuates as it interacts with the electrons and nuclei of the target material. When a beam of fast ions is passed through matter, the charge-changing interactions that take place in the target will result in a distribution of charge states in the emerging beam. Knowledge of the equilibrium charge distribution of ions emerging from matter is important not only for an understanding of atomic collision physics, but also for practical purposes such as the design of nuclear instruments and accelerators. The study of equilibrium charge distributions obtained by passing highly energetic, heavy ions through foils reveals important information about their interaction with matter. This information can be applied to predict the damaging effects of heavy ions on systems ranging from biological molecules to semiconductor devices.

Equilibrium charge state distributions have been investigated for many years, and a variety of data compilations devoted to the subject exist[1,2]. However, new technologies have recently made it possible to create ion beams of much higher energies than were previously attainable. Past studies have concentrated mainly on lower energy regions. Considering the recent increase in applications of heavier and faster ions in various fields, a need has developed for information on the charge state distributions for ions in higher energy regions. Recent studies have pointed out the need for information in higher energy regions[3,4], but thus far no major comprehensive investigations have been undertaken.

The objective of this project is to determine the charge state distributions that result when heavy, highly energetic Xe ions are passed through matter. Specifically, the interaction of 8 MeV/μ Xe^{21+} with carbon foils of varying thickness was investigated. The resulting charge state distributions were compared to those theoretically predicted by semi-empirical formulas based on lower energy studies and a new phenomenon was discovered concerning the charge distributions resulting from the traversal of two foils.

II. Background

A. Previous Work

Investigations of charge state distributions have been carried out for over 70 years. During this time, a large amount of data has been amassed covering a wide range of projectile energies, atomic numbers, and target materials. Many semi-empirical formulas have been proposed to explain this data[5,6,7,8]. Recent experimental activity has focused more on higher energy ranges and has included heavier projectiles. Considerable effort has been devoted to the development of semi-empirical relationships to describe this data. Some of these equations, most notably those proposed by Baron[5], Sayer[6], Nikolaev-Dimitriev[7], and Shima[8], have been quite good at predicting results in a fairly wide energy region. However, studies have indicated that as the projectile atomic number and energy is increased, the results tend to deviate from predictions[4]. More specifically, Martin warned that the existing charge state formulas should be used with caution for projectile ions with $Z > 36$ and energies above 1 MeV/μ and pointed out the need for more data in this range.

B. Theory

The charge of a fast ion moving through matter fluctuates as a result of electron loss and capture in collisions with the target atoms. When a fast moving heavy ion collides violently with a multielectron target atom, some of the translational energy of the ion is transferred to the electrons of both the target and the projectile. In comparatively rare events, the charged particle will interact with the nucleus, but since atoms are much larger than nuclei, collisions with electrons are far more probable. When energy is transferred to the electrons, they are raised to excited states and, if the energy is sufficient, ionized. As the incident ion passes through the target, it loses a little energy to the target atom electrons with each collision. When the ion enters the target, its velocity is so high that it primarily experiences electron loss. However, as the ion loses energy and slows down, it begins to capture electrons. Thus, as energetic ions pass through a medium their charges vary as a function of the penetration depth. After a sufficient number of collisions, the competing processes of electron loss and capture in the projectile ion will reach an equilibrium state in which the rates of the two processes are approximately equal and thus the distribution of charge states in the material will become effectively constant. The charge state distribution established at this point is called the equilibrium charge state distribution, and it depends only on the projectile ion species, the ion velocity, and to a minor extent the nature of the target. The equilibrium charge state distribution is independent of the initial charge of the ion. The point at which equilibrium is reached in a given material is called the equilibrium thickness of the material.

The charge state distribution is specified by the relative fraction of ions, $F(q)$, in each charge state. The charge state distribution can be approximated by a Gaussian distribution

$$F(q) = \frac{1}{d\sqrt{2\pi}} \exp\left[-\frac{1}{2}\left(\frac{q-\bar{q}}{d}\right)^2\right]$$

Where q is the average charge, defined by

$$\bar{q} = \sum_q \{qF(q)\}.$$

The mean charge is represented by the centroid of the Gaussian distribution. The distribution is characterized by $\bar{q}$ and d, where d is the distribution width (or standard deviation) of the Gaussian. As the thickness of the target is increased, the $\bar{q}$ of the distribution increases until the equilibrium thickness of the material is reached. Beyond this point, increasing the target thickness has no further effect on the mean charge until the energy of the ion begins to change significantly.

Various semi-empirical formulas have been developed to predict $\bar{q}$ and d for equilibrium charge state distributions. The most widely used of these equations are shown below.

Baron[5]:

$$\bar{q} = Z\left[1 - C\exp\left(-\frac{386}{Z^{0.447}}\sqrt{W}\right)\right]$$

$$d = d_0\left[\bar{q}\left(1 - \frac{\bar{q}}{Z}\right)^{\frac{1}{k}}\right]^{\frac{1}{2}}$$

where

W = energy (Mev/μ)

Z = atomic number

Shima[8]:

$$\bar{q} = Z^{\bullet}\left[1 - e^{-1.25Y + 0.32Y^2 - 0.11Y^3}\right]$$

$$Y = \frac{\beta}{0.012Z^{0.45}}$$

$$\beta = \frac{\sqrt{\gamma^2 - 1}}{\gamma} \qquad \gamma = 1 + \frac{W}{E_o}$$

Nikolaev-Dimitriev[7]*:*

$$\bar{q} = Z\left[1+\left(\frac{\upsilon}{\upsilon' Z^{a}}\right)^{-\frac{1}{k}}\right]^{-\frac{1}{2}}$$

Sayer[6] has proposed an alternative to the strictly Gaussian distribution given by

$$F(q) = \frac{1}{S}\exp\left[-\frac{1}{2}\left(\frac{q-q_o}{d}\right)^2 \frac{1}{1+R(q-q_o)}\right]$$

$$S = \sum_{q=1}^{Z}\exp\left[-\frac{1}{2}\left(\frac{q-q_o}{d}\right)^2 \frac{1}{1+R(q-q_o)}\right]$$

$$q_o = Z\left[1-1.03\exp\left(-47.3Z^{-0.38}\beta^{0.86}\right)\right]$$

$$d = 0.47Z^{0.46}\left[\frac{q_o}{Z}\left(1-\frac{q_o}{Z}\right)\right]^{0.26}$$

$$R = 0.0007Z - 0.7\beta \qquad \beta = \frac{\upsilon}{c}$$

III. Experimental Methods

The experimental setup is shown in Figures 1 and 2. The entire apparatus is held under high vacuum to limit scattering and unwanted interactions with gas molecules. The K500 superconducting cyclotron accelerates ions to produce a beam of 8 MeV/μ Xe^{21+}. The beam emerges from the cyclotron and passes through a collimator that defines the beam to 1 mm in diameter. The beam proceeds through a carbon foil in a remotely controlled target wheel. The target wheel is not pictured in the diagram. It replaced the gas cell pictured in the diagram. The target wheel has spaces for many different targets so that foils of different thickness could be tested without breaking the vacuum. The thickness (given in μg/cm^2, where 1 μg/cm^2 $\approx$ 4 x 10^{-7} cm) of a random sampling of the foils was verified by an independent a-particle energy loss experiment. After passing through the target foil, the beam proceeded on through a bending magnet, where the magnetic field of the bending magnet, B, dispersed the ions through trajectories that depended on their charges according to the equation for radius of curvature

$$R = \frac{mv}{qB}$$

where

m = mass of ion

v = velocity of ion

Thus the bending magnet spatially differentiated the different charge states. This charge differentiated beam then impinged on a position sensitive microchannel plate detector system (PSD), which enabled charge identification by measuring the impact position of each ion (see Figure 3). The output from the detector was digitized and sent to a computer for analysis. The information from the PSD was used to create a plot of the number of particles present in each charge state.

IV. Data Analysis and Results

A. Data Analysis

The data from the foil runs consisted of the number of detected particles per channel, where the channel number was directly proportional to the impact position of the particle. This data was accumulated in a multichannel analyzer and plotted on a CRT screen as shown in Figure 4.

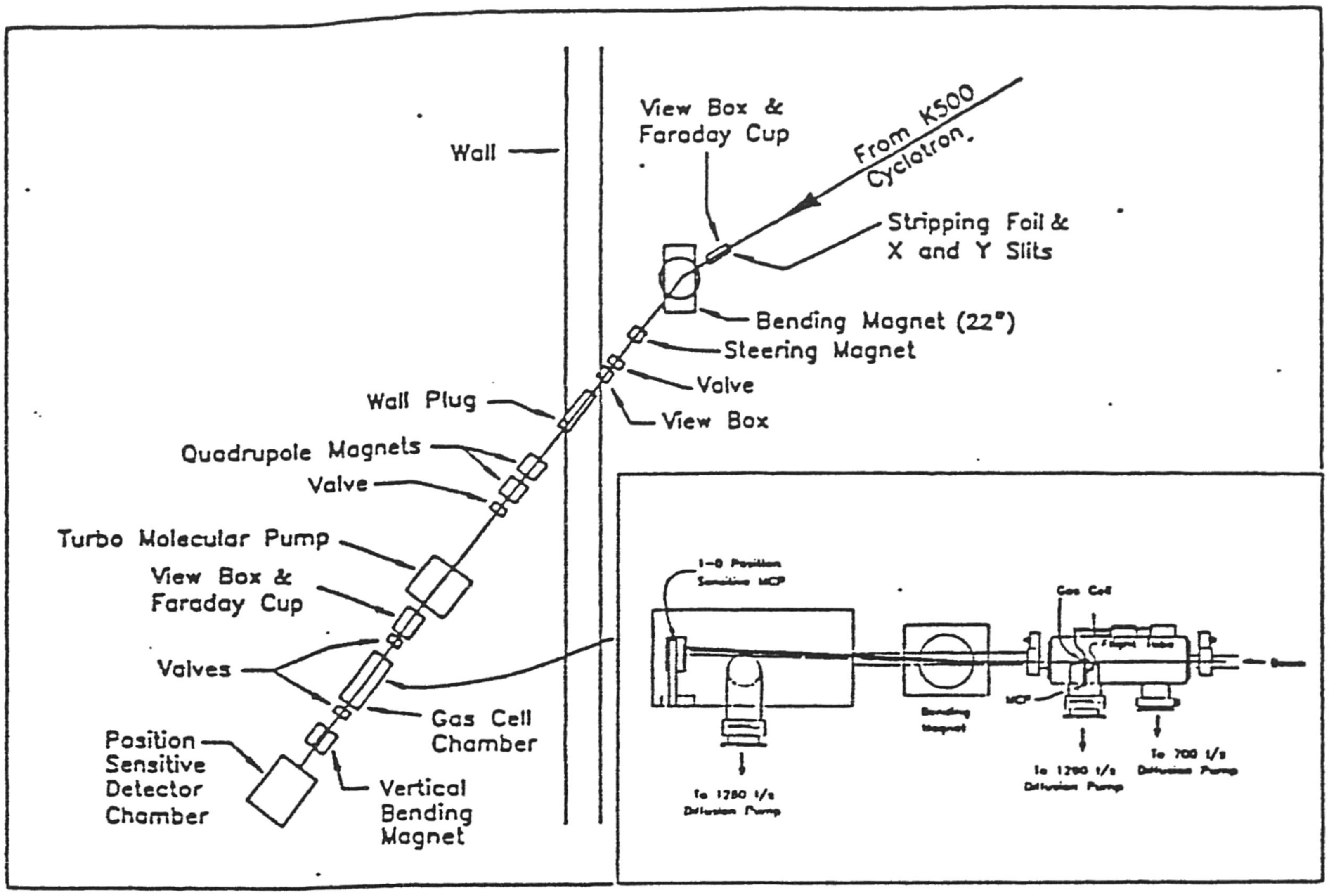

Figure 1. Beam line for carbon foil experiment.

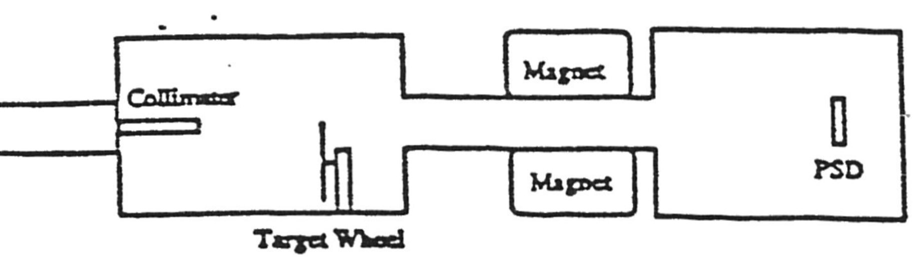

Figure 2. Close-up view of collimator, target wheel, bending magnet, and PSD.

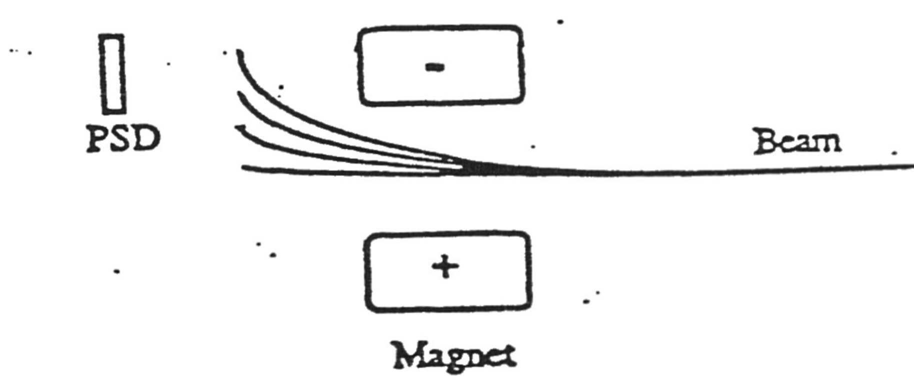

Figure 3. Effect of magnet on positive ions of differing charge.

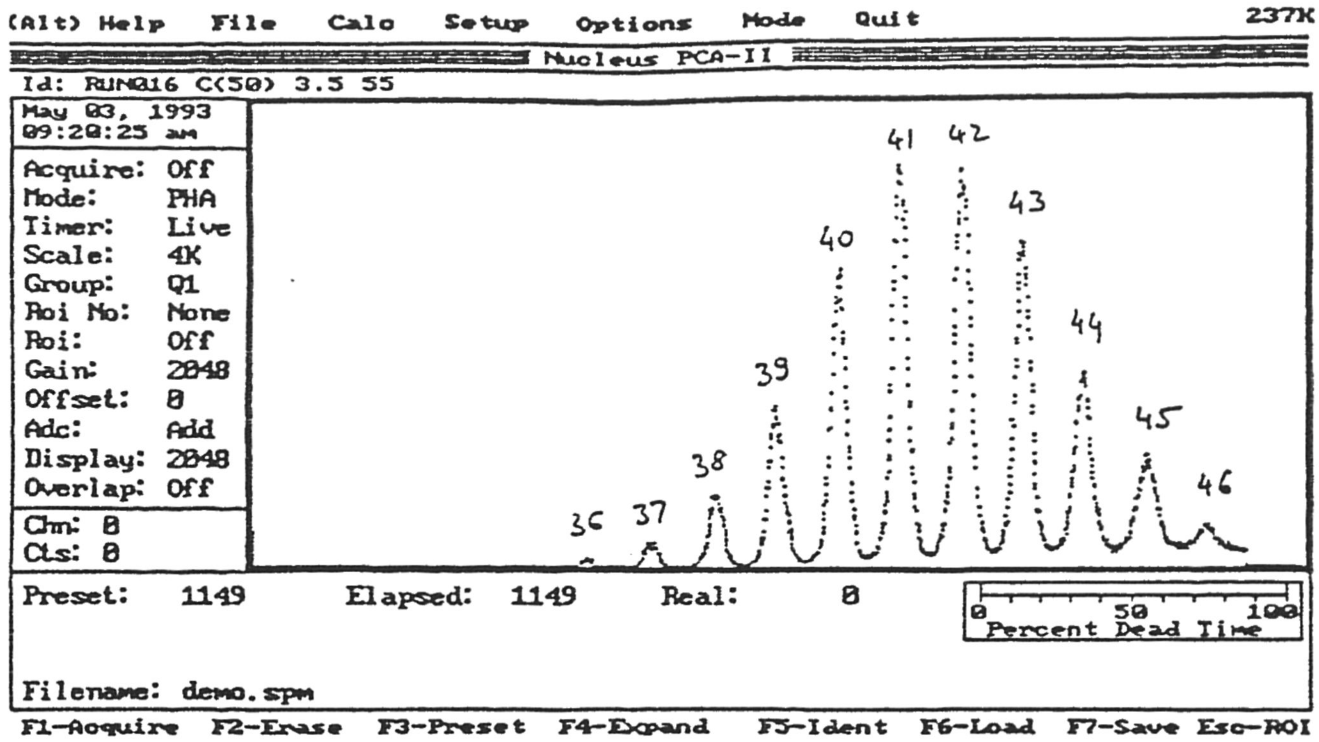

Figure 4. Accumulated spectrum from carbon foil run on multi-channel analyzer.

The first step in the analysis of data was to identify the charge state corresponding to each peak in the position spectrum. One measurement was performed without a target, so that only the incident beam of Xe^{21+} was impinging on the detector. The centroid of the predominant peak in this distribution therefore corresponded to the Xe^{21+} charge state, and the peaks in the other measurements with target foils all were identified using the Xe^{21+} peak as a calibration point. The data was then converted into a different file format on the VAX computer system and read into a nonlinear least-squares spectral analysis program FACELIFT. The peaks of the spectra were fit with Gaussian functions having variable centroids, areas, and standard deviations. The next step in the data analysis was to compute $\bar{q}$ for each foil thickness. This was accomplished by entering the centroid and area of the peak of each charge state, as determined by FACELIFT, into a spreadsheet file. Before further analysis, the peak areas had to be corrected for the efficiency of the PSD, which varied with position (channel number). The correction factor for each peak was calculated with a formula obtained from an analysis of calibration data. The corrected area of each peak was determined by dividing the original area by the efficiency correction factor. The fraction that each charge peak comprises of the total area was then determined by the equation

$$F(q) = \frac{A_q}{A_{tot}}$$

where A_q is the area of the individual charge peak and A_{tot} is the sum of the areas of each charge peak in the distribution. The average charge of the distribution was calculated using the formula

$$\bar{q} = \sum_q \{qF(q)\}$$

In order to determine the equilibrium $\bar{q}$ and the foil thickness at which equilibrium was reached, a plot was made of the average charge versus foil thickness (see Figure 5). In this figure, it is apparent that there is an anomaly at three thicknesses where two data points appear. At these thicknesses, double foils were employed. The two foils (of different thickness) were put together in the target wheel and the charge state distribution was measured for two orientations with respect to the beam - one with the thinner foil upstream (closer to the incoming beam) and one with the thicker foil upstream. The data indicates that these two orientations produce different charge state distributions. This is a very interesting and unexpected effect which has, to our knowledge, not been observed before. From this point on, the single foil data and the double foil data will be discussed separately.

B. Single Foil Results

In order to get the equilibrium average charge, another plot of average charge versus thickness was constructed, using only the single foil data (see Figure 6). It can be seen from Figure 6 that the average charge increases as the thickness increases until it approaches equilibrium, at which point the curve levels off. By averaging the $\bar{q}$ values of the four thickest foils, the equilibrium

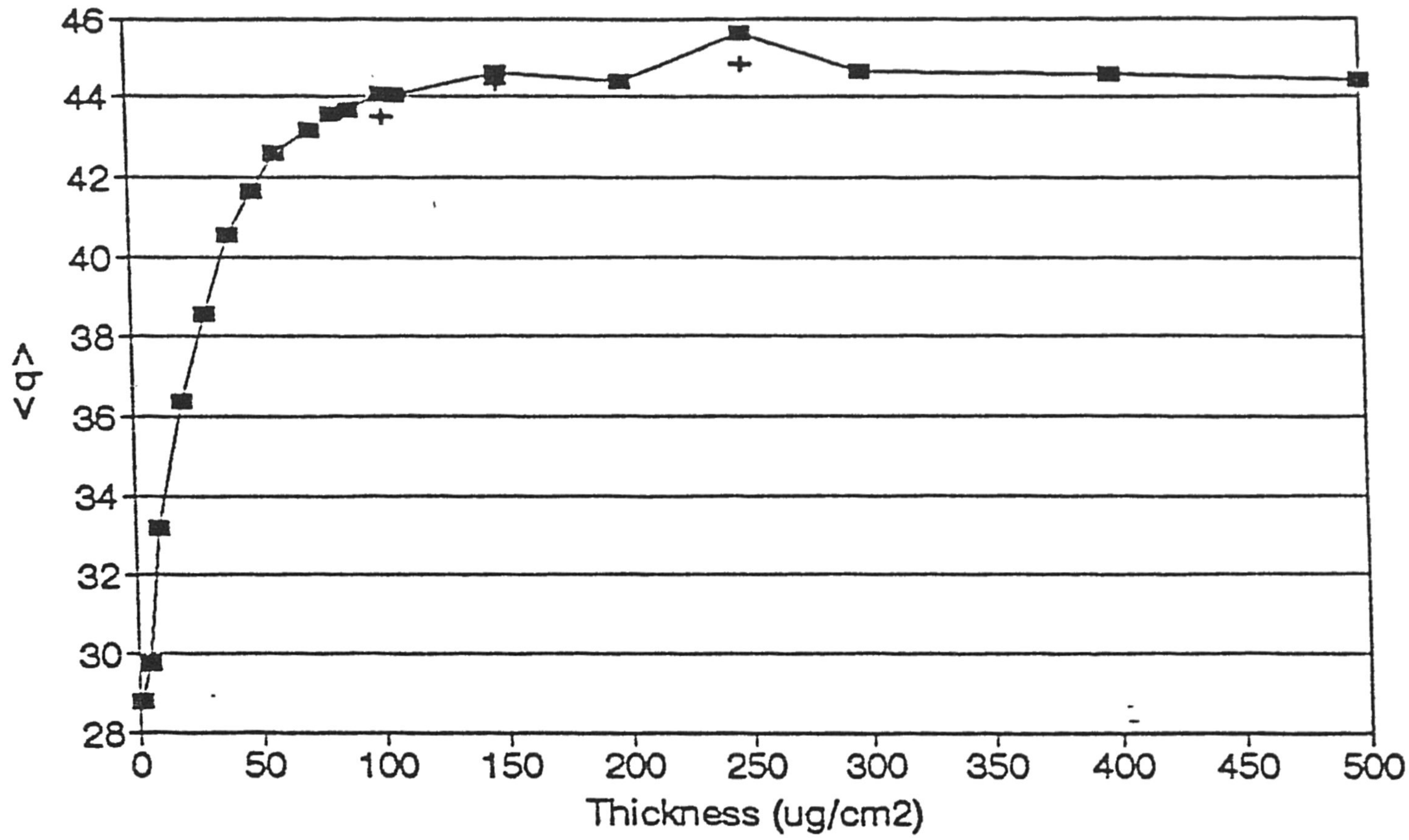

Figure 5. Thickness dependence of $\bar{q}$ for all carbon foils.

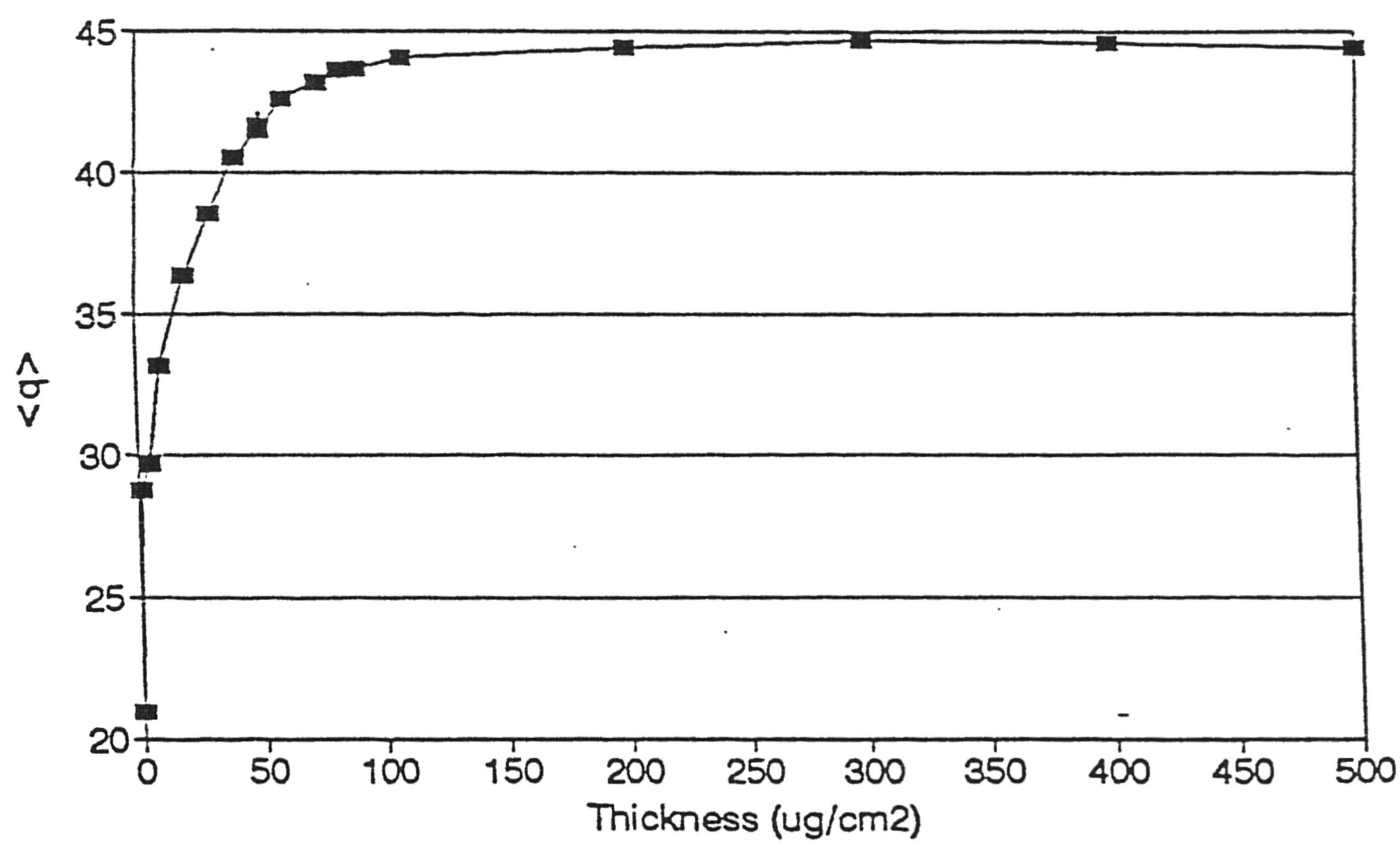

Figure 6. Thickness dependence of $\bar{q}$ for single carbon foils.

average charge was determined to be $\bar{q} = 44.50^{+} \pm .32$. The equilibrium foil thickness was then found by determining the point at which the curve first reaches the equilibrium average charge. A value of approximately 240 μg/cm^2 was obtained for the equilibrium foil thickness. Figures 7-10 show the fitted spectra and charge state distributions associated with four of the points along the curve of Figure 6. These include two points for relatively thin foils, and a point immediately before and after the equilibrium foil thickness is reached. It is evident from these figures that as the foil thickness increases, the peaks in the distribution tend to get wider as a result of increased (multiple) scattering and energy loss. As a result, the thicker foil spectra were harder to fit, but it was still possible to extract accurate results from these spectra using FACELIFT.

C. Double Foil Results

Two different experiments were performed on double foil targets. The first experiment, discussed earlier, was performed in conjunction with an investigation of the thickness dependence of the average charge emerging from carbon foils. The second experiment, undertaken after the double foil effect was discovered in the original experiment, focused on determining what variables affect the charge distributions emerging from double foils. The results of the two experiments will be discussed separately.

1. First Experiment:

The three double foils used were 30+74 μg/cm^2, 60+90 μg/cm^2, and 50+200 μg/cm^2. Superimposed charge distributions for the two orientations of each double foil set are shown in Figures 11-13. Clearly the distributions and average charges of the two orientations of the double foils

(a)

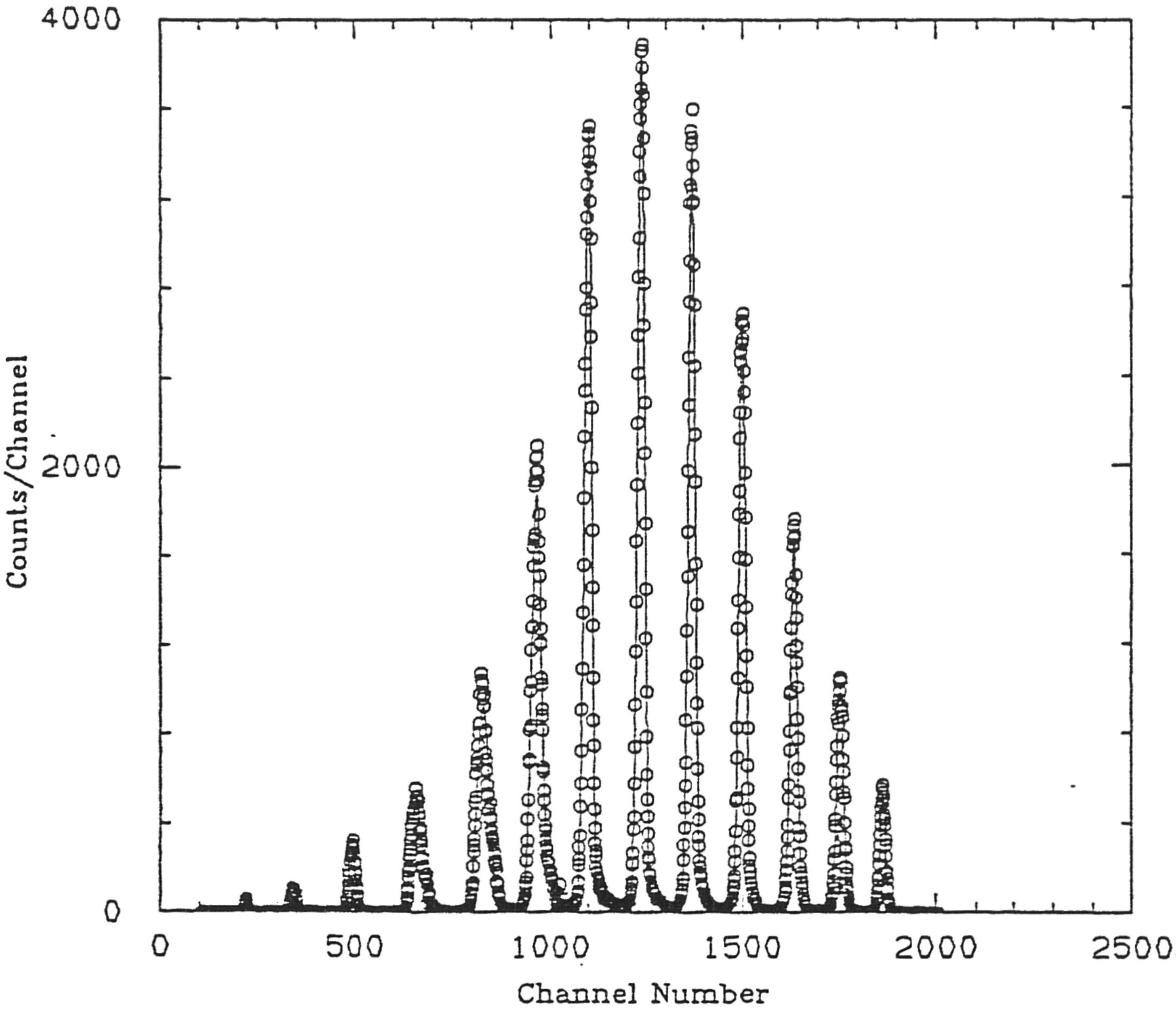

(b)

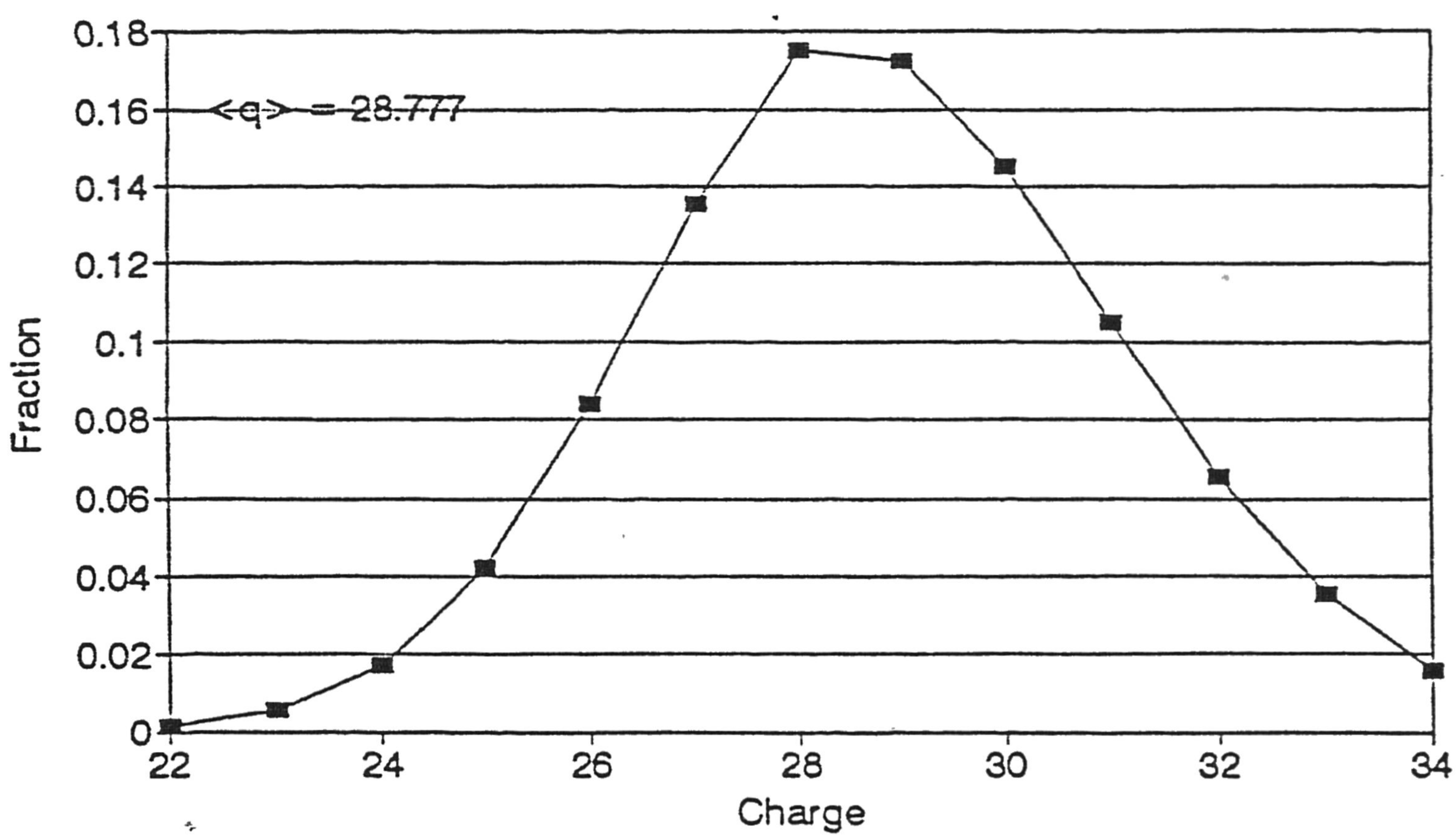

Figure 7. (a) Fitted spectrum and (b) charge state distribution for 1.2 μg/cm² carbon foil.

(a)

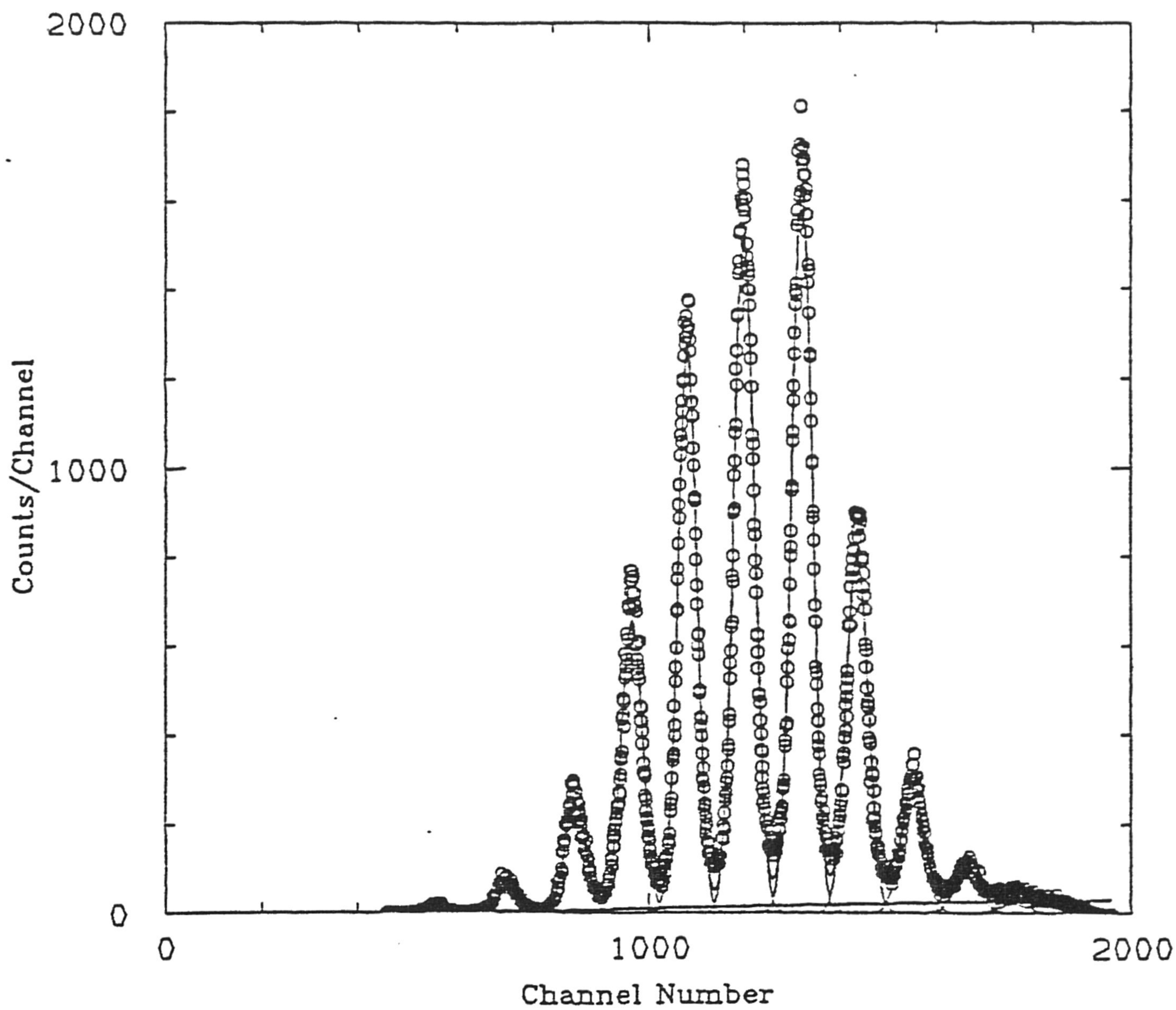

(b)

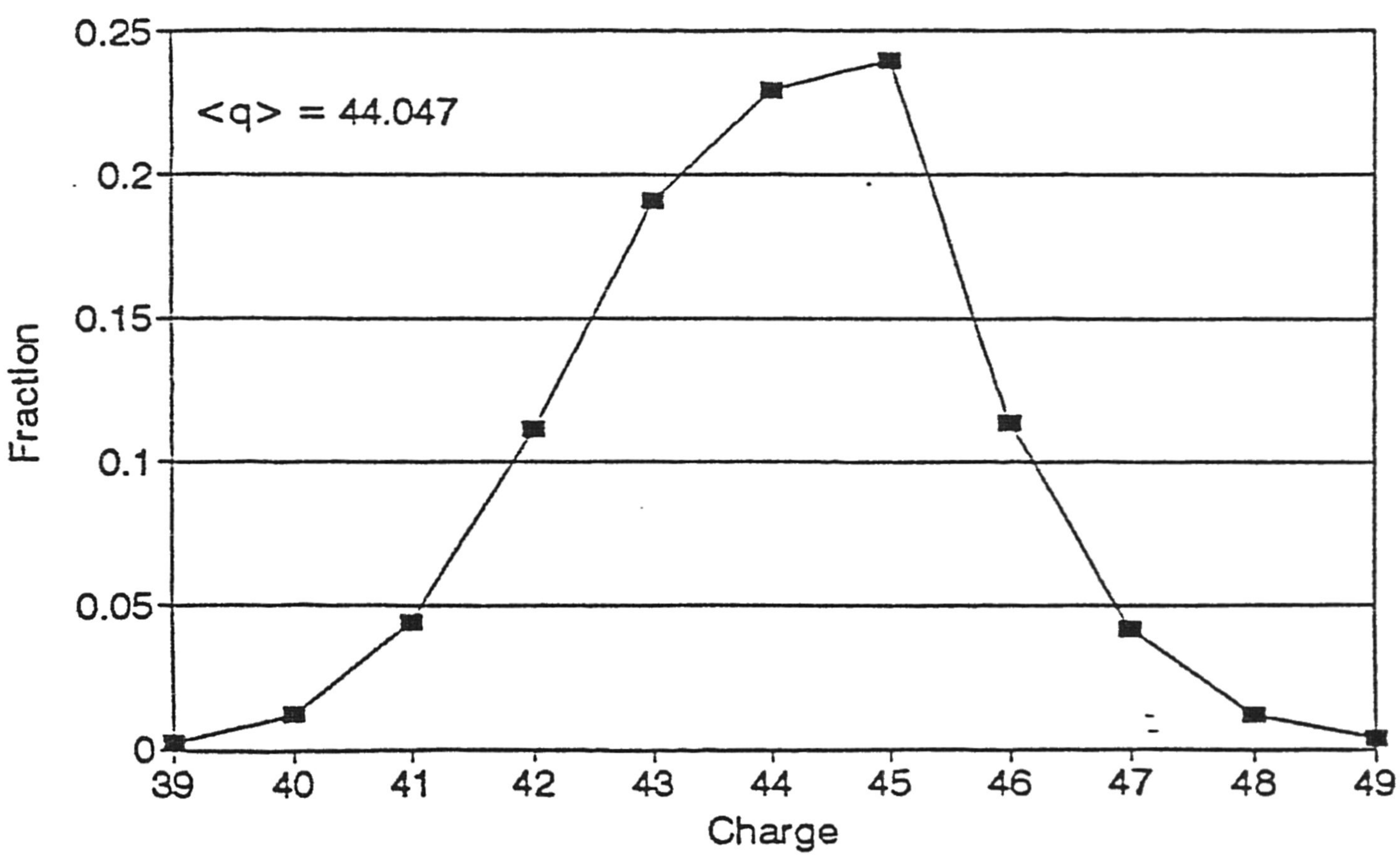

Figure 8. (a) Fitted spectrum and (b) charge state distribution for 109 $\mu g/cm^2$ carbon foil.

(a)

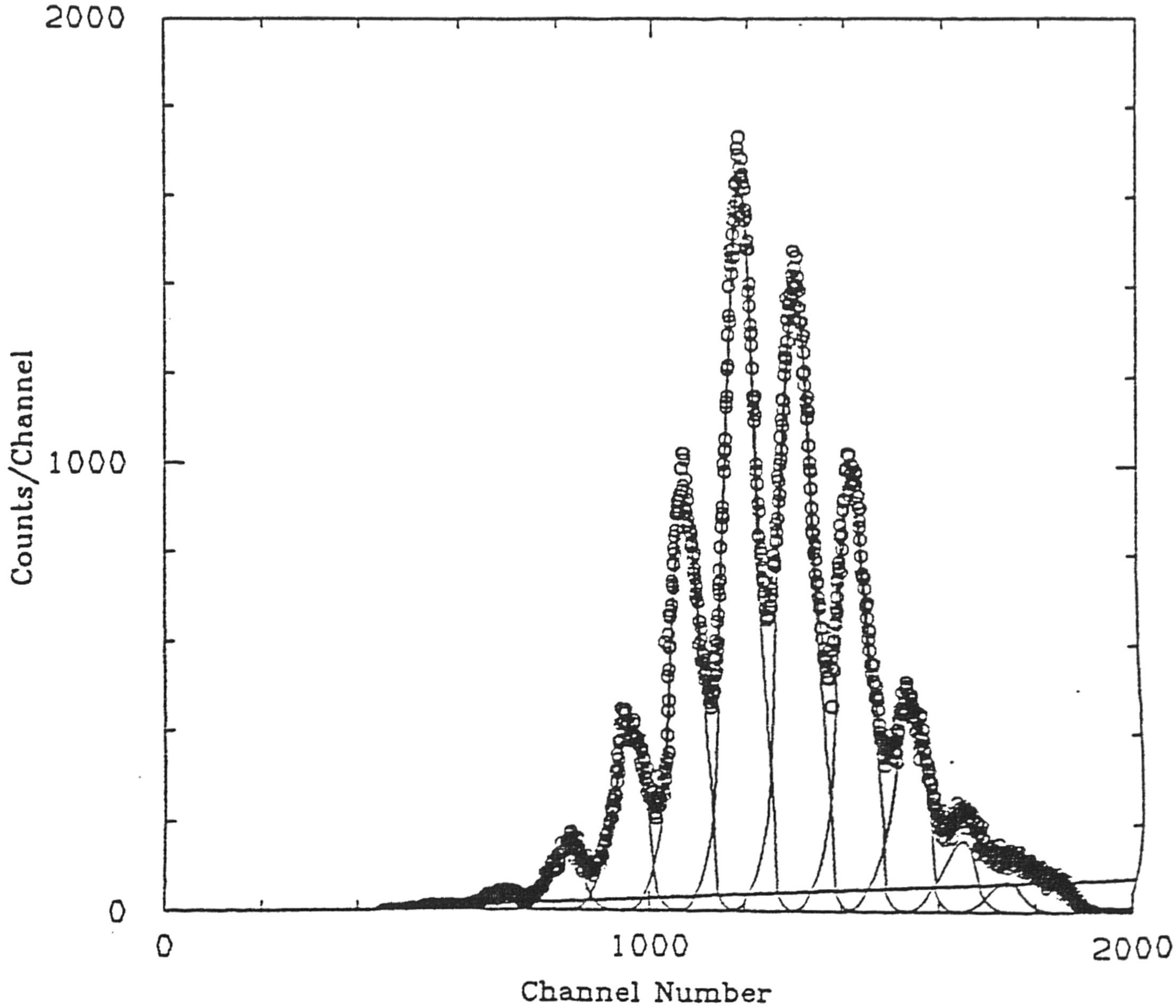

(b)

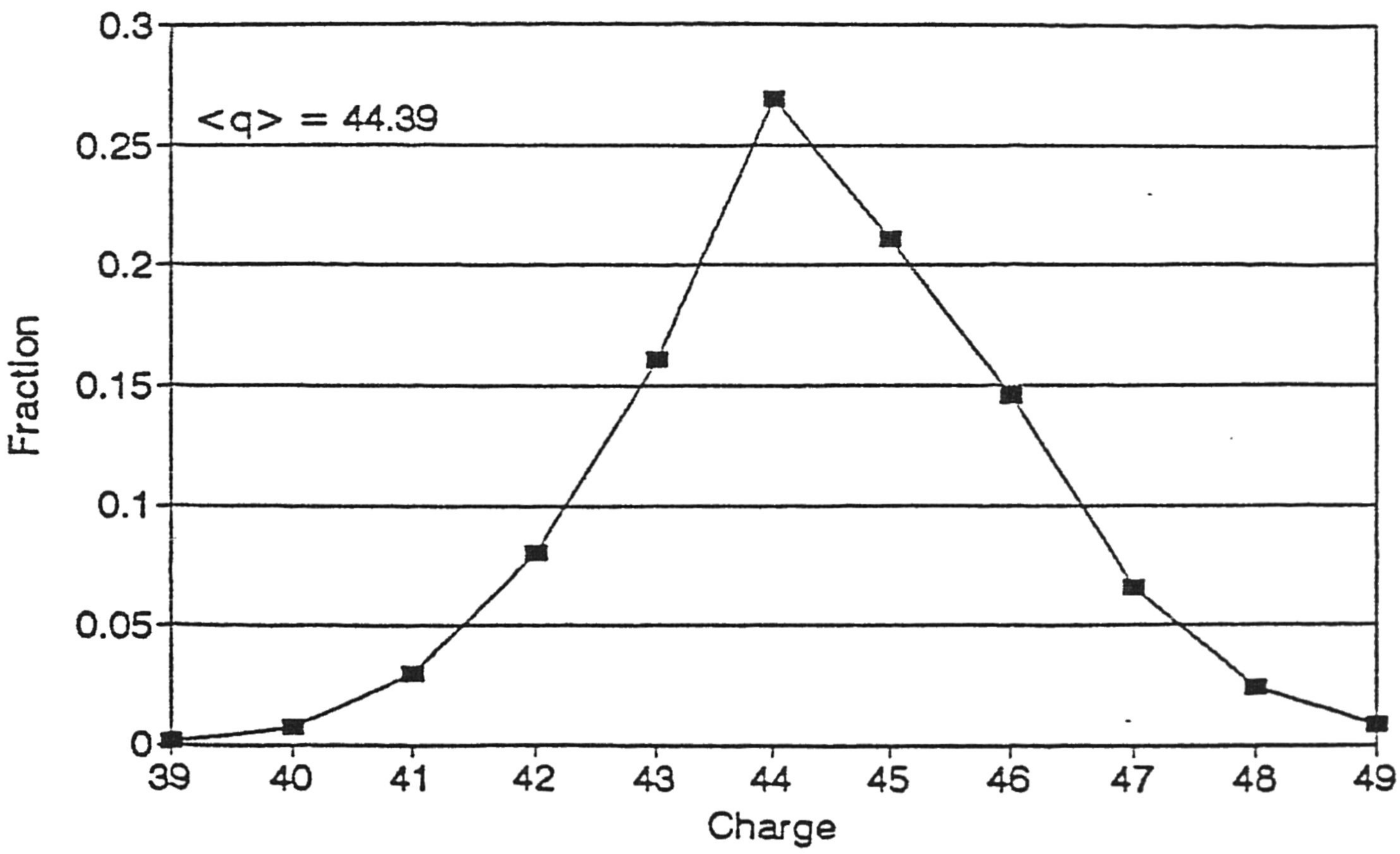

Figure 9. (a) Fitted spectrum and (b) charge state distribution for 200 μg/cm² carbon foil.

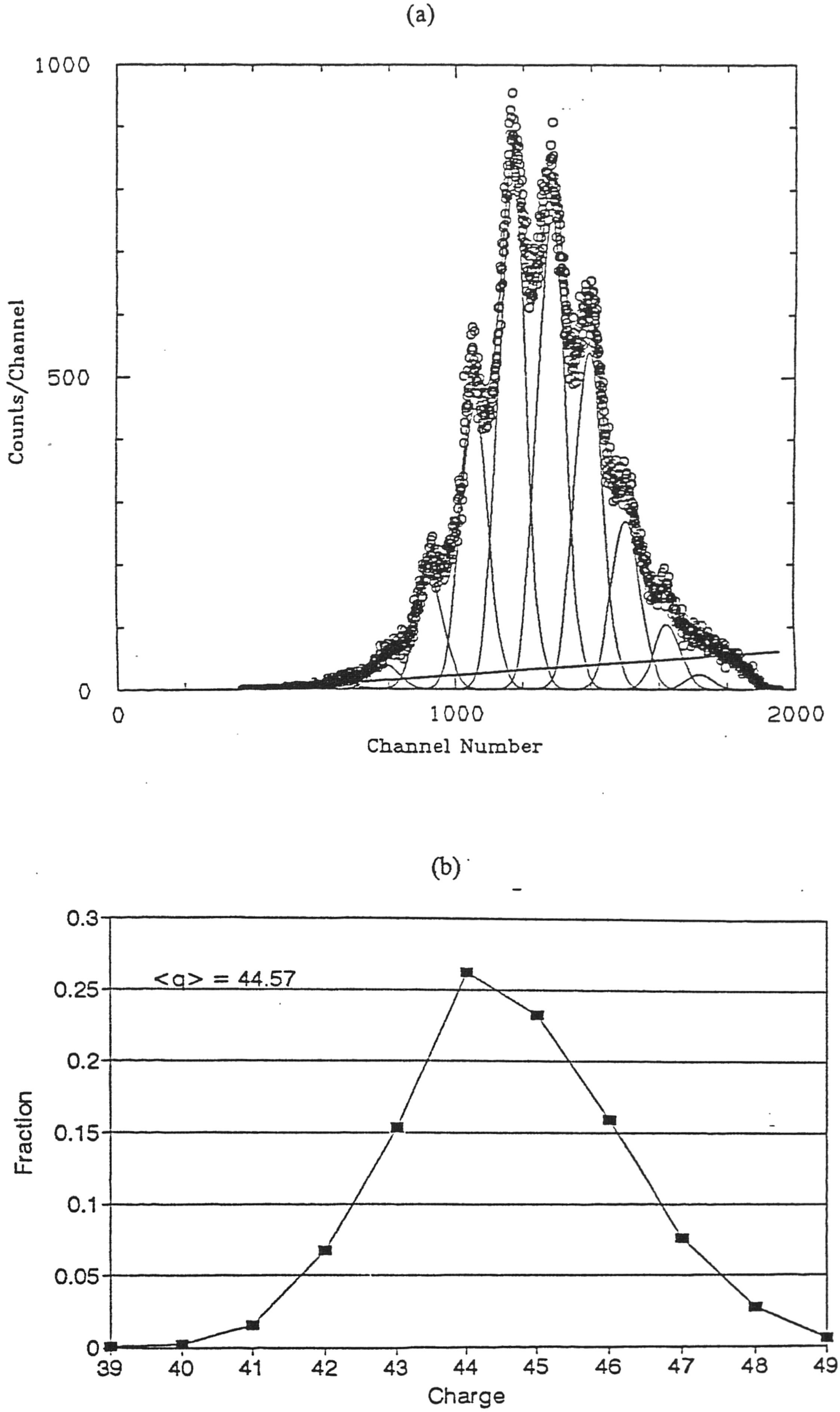

Figure 10. (a) Fitted spectrum and (b) charge state distribution for 400 $\mu g/cm^2$ carbon foil.

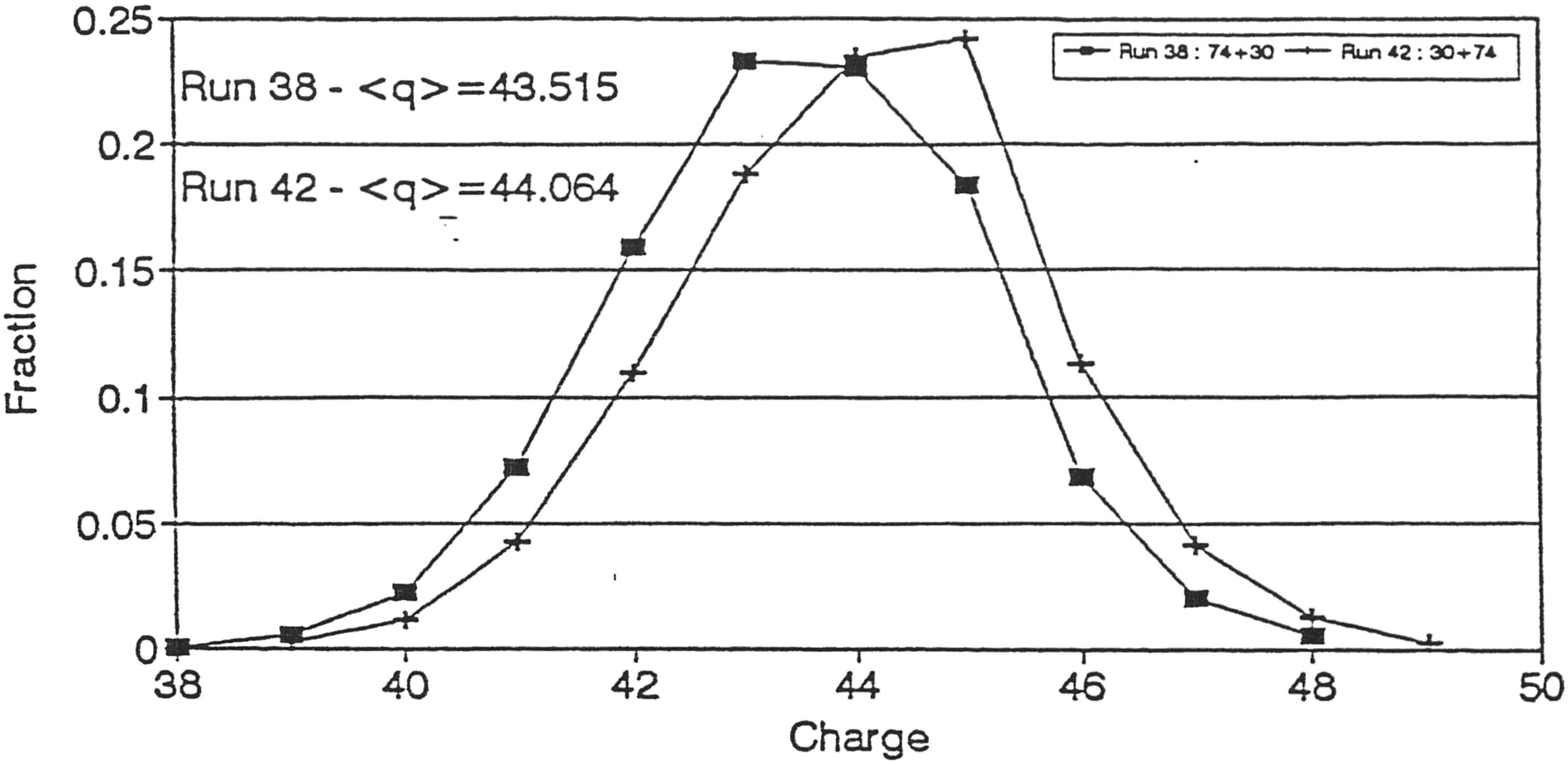

Figure 11. Superimposed charge state distributions for 30+74 μg/cm² double foil. Foil orientation is written as 'upstream foil + downstream foil'.

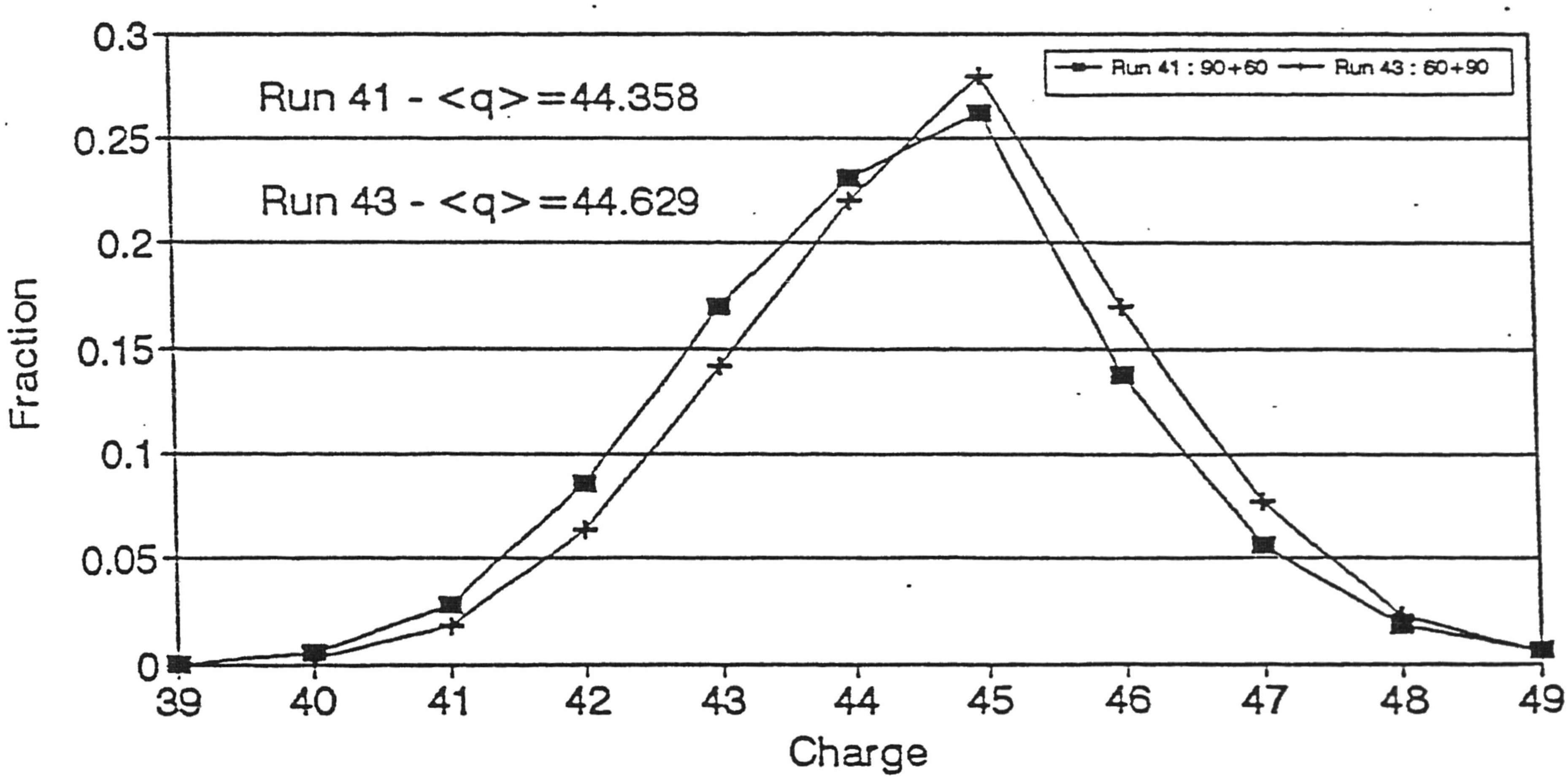

Figure 12. Superimposed charge state distributions for 60+90 μg/cm² double foil. Foil orientation is written as 'upstream foil + downstream foil'.

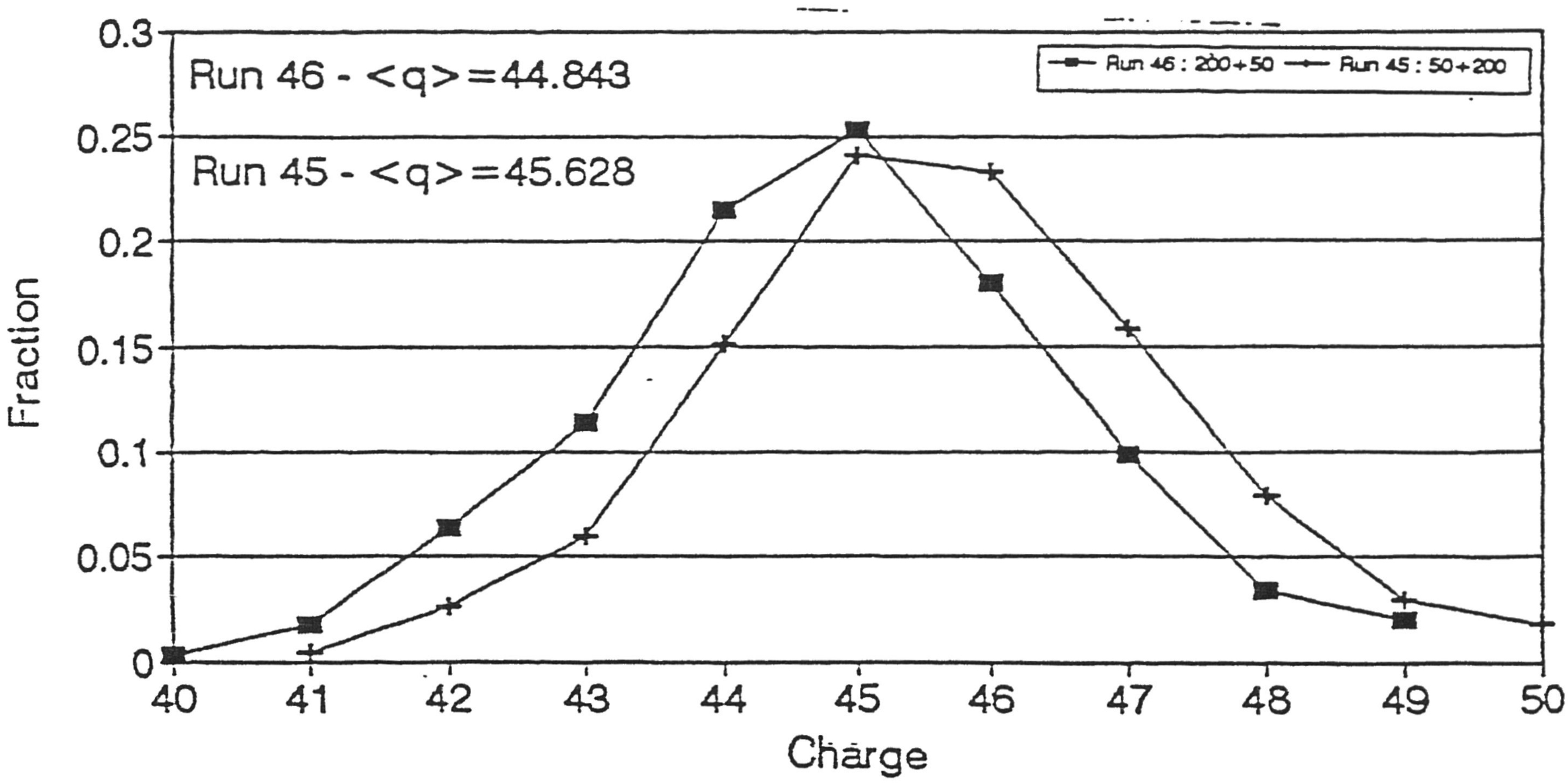

Figure 13. Superimposed charge state distributions for 50+200 μg/cm² double foil. Foil orientation is written as 'upstream foil + downstream foil'.

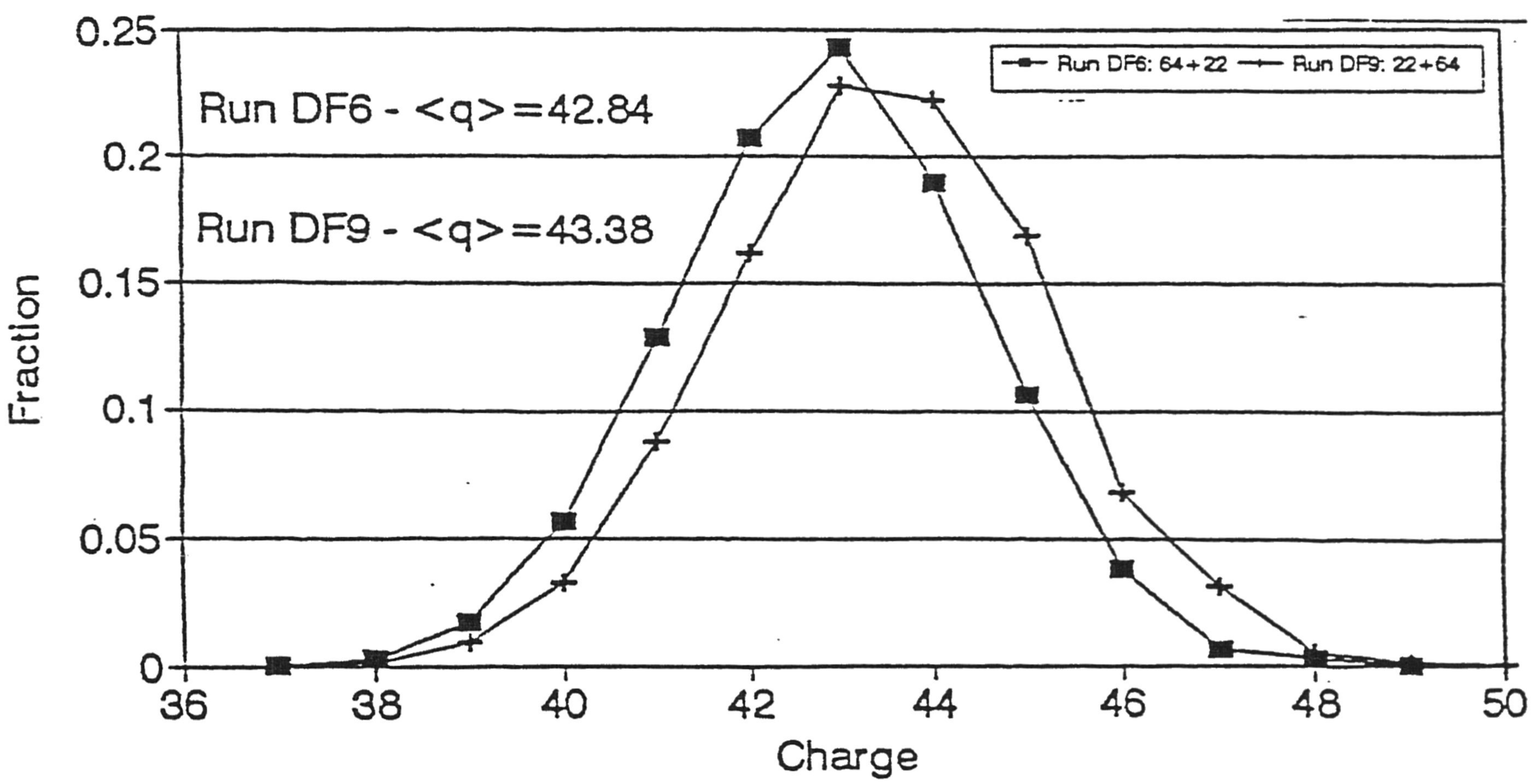

Figure 14. Superimposed charge state distributions for 22+64 μg/cm² double foil. Foil orientation is written as 'upstream foil + downstream foil'.

are different. In addition, it is evident that the orientations with the thinner foil upstream have uniformly higher average charges than the opposite orientation.

2. Second Experiment

This experiment was performed with one double foil, 22+64 $\mu g/cm^2$, and one single foil, of thickness 84 $\mu g/cm^2$ (close to the sum of the thickness of the two components of the double foil). A group of six runs was performed with the 84 $\mu g/cm^2$ foil, three with the foil in one orientation and three with the foil in the other orientation. The averages of the two groups of three runs differed by less than .05%, indicating that the orientation of a single foil has no significant effect on the charge state distribution. Another group of six runs was performed using the 22+64 $\mu g/cm^2$ double foil, three with the thinner foil upstream and three with the thicker foil upstream. The same orientation effect discovered in the previous experiment was observed for the two different orientations (see Figure 14). Additional runs were executed testing the effect of different separations between the two foils ranging from approximately 0.1 mm to 3 mm. The largest difference observed was ~.3% between the resulting average charge, indicating that the separation between the foils does not significantly affect the charge distribution.

V. Discussion

A. Single Foil

Despite predictions to the contrary, the equilibrium average charge obtained in this experiment for 8MeV/μ Xe^{21+} incident on carbon foils agrees well, within ±1 charge state, with the semi-empirically predicted equilibrium average charges. The theoretically predicted charge distributions are equilibrium charge distributions, and thus should be compared only to experimental charge distributions corresponding to thicknesses above 240 μg/cm^2. The superposition of the various theoretically predicted equilibrium charge state distributions and the corresponding predicted equilibrium average charge with the measured charge state distribution obtained for the 300 μg/cm^2 foil are shown in Figures 15-18. These figures show that both the charge state distribution and the average charge obtained from the 300 μg/cm^2 foil are best matched by the Nikolaev-Dimitriev semi-empirical formula.

In order to describe the evolution of the average charge with respect to foil thickness (see Figure 6), a model was developed. The following boundary conditions determined the form of the model equation for average charge as a function of target thickness: (1) the predicted average charge must equal the charge of the incoming beam as the thickness of the foil approaches zero, (2) the predicted average charge must equal the equilibrium average charge and be independent of the initial charge state as the thickness of the foil approaches infinity, and (3) the model must include a term related to charge change occurring after the beam has exited the foil. The last condition is necessary because previous studies have shown[3,9] that the average charge of the beam actually increases after leaving the target. This charge change, usually corresponding to a few charge units, results from the Auger decay of inner-shell vacancy states in the exiting ions. In Auger decay, an inner shell electron vacancy is filled by an electron from a higher shell. The energy gained in this transition then results in the expulsion of another electron from the ion. Hence one Auger decay increases the positive ionic charge by one unit. The probability of post-foil charge increase therefore depends on the distribution of inner-shell vacancies in the emerging projectile ion. Auger decay occurs outside the foil because the inner shell vacancies have mean lifetimes that are longer than the time it takes the ion to traverse the target. From independent x-ray

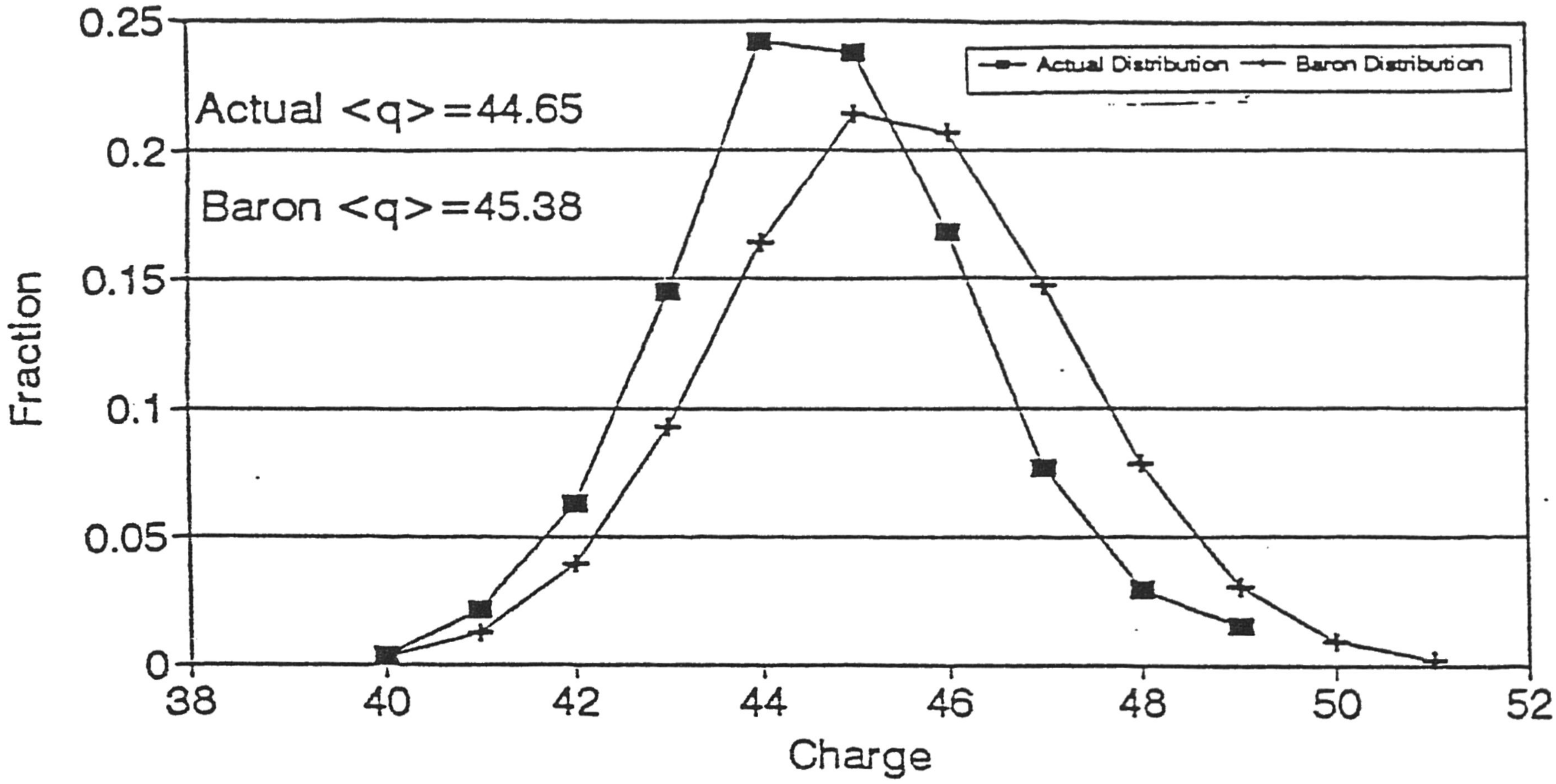

Figure 15. Baron semi-empirical distribution superimposed on measured distribution for 300 $\mu g/cm^2$ carbon foil.

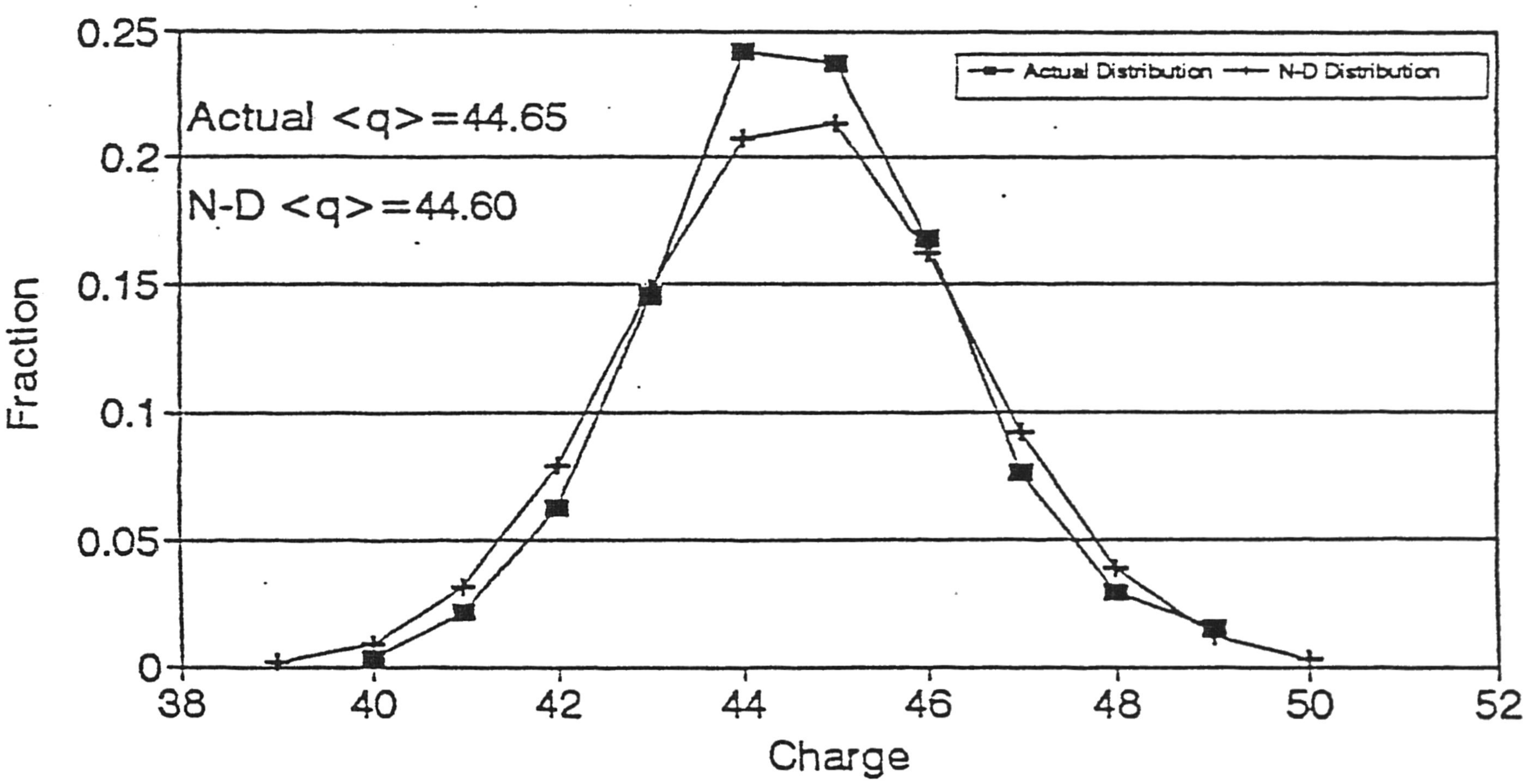

Figure 16. Nikolaev-Dmitriev semi-empirical distribution superimposed on measured distribution for 300 $\mu g/cm^2$ carbon foil.

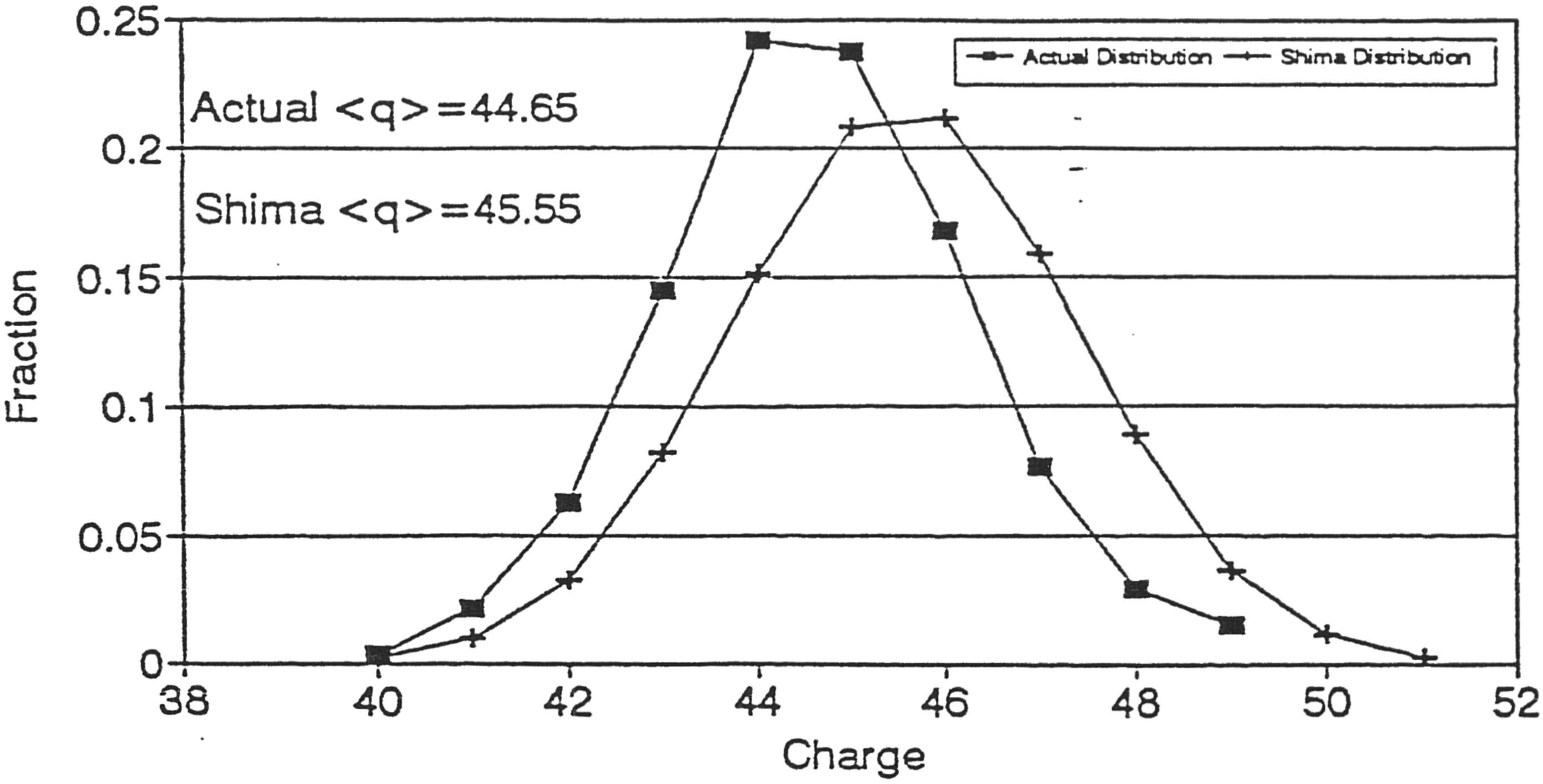

Figure 17. Shima semi-empirical distribution superimposed on measured distribution for 300 μg/cm^2 carbon foil.

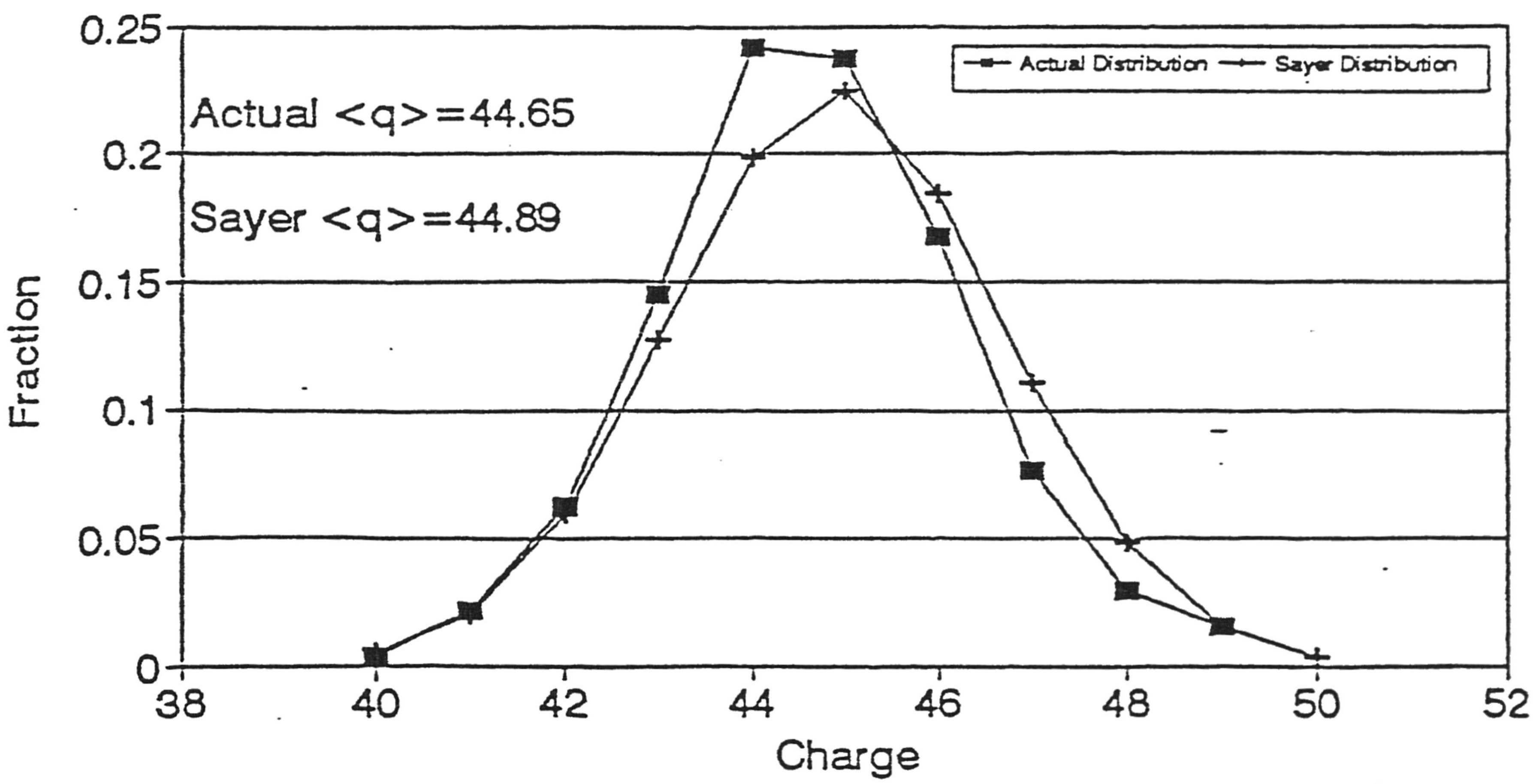

Figure 18. Sayer semi-empirical distribution superimposed on measured distribution for 300 μg/cm^2 carbon foil.

experiments, it was determined that the outermost electrons are distributed between the L and M-shells, with an average of 5 electrons in the L-shell once the ions have reached charge state equilibrium. It was also determined that the average equilibrium charge increases by approximately 3 units after the ion exits the foil.

The model proposed for the evolution of the average charge with foil thickness is

$$\langle q \rangle_o = q_E(1 - e^{-at}) + q_I e^{-at} + \Delta Q(1 - e^{-bt})$$

where

$<q>_o$ = average charge outside foil

q_E = equilibrium charge inside foil

q_I = incident charge

ΔQ = charge change upon exiting foil at equilibrium

a,b = constants

The parameters of this model (q_E, ΔQ, a, and b) were determined by fitting the above equation to the equilibrium charge versus foil thickness data using the program SigmaPlot[10]. In one fit, all the parameters were allowed to vary except for q_I, which was set equal to 21^+. The results of this fit are shown in Figure 19. Although this fit recreates the data very accurately, it does not yield a physically realistic value for the charge change parameter (ΔQ = 16.72). In the other fits, both q_I and ΔQ were fixed. The fit for ΔQ=3 is shown in Figure 20. Although this fit does not recreate the data as accurately as the first fit, it is a good fit and is physically reasonable. The value of

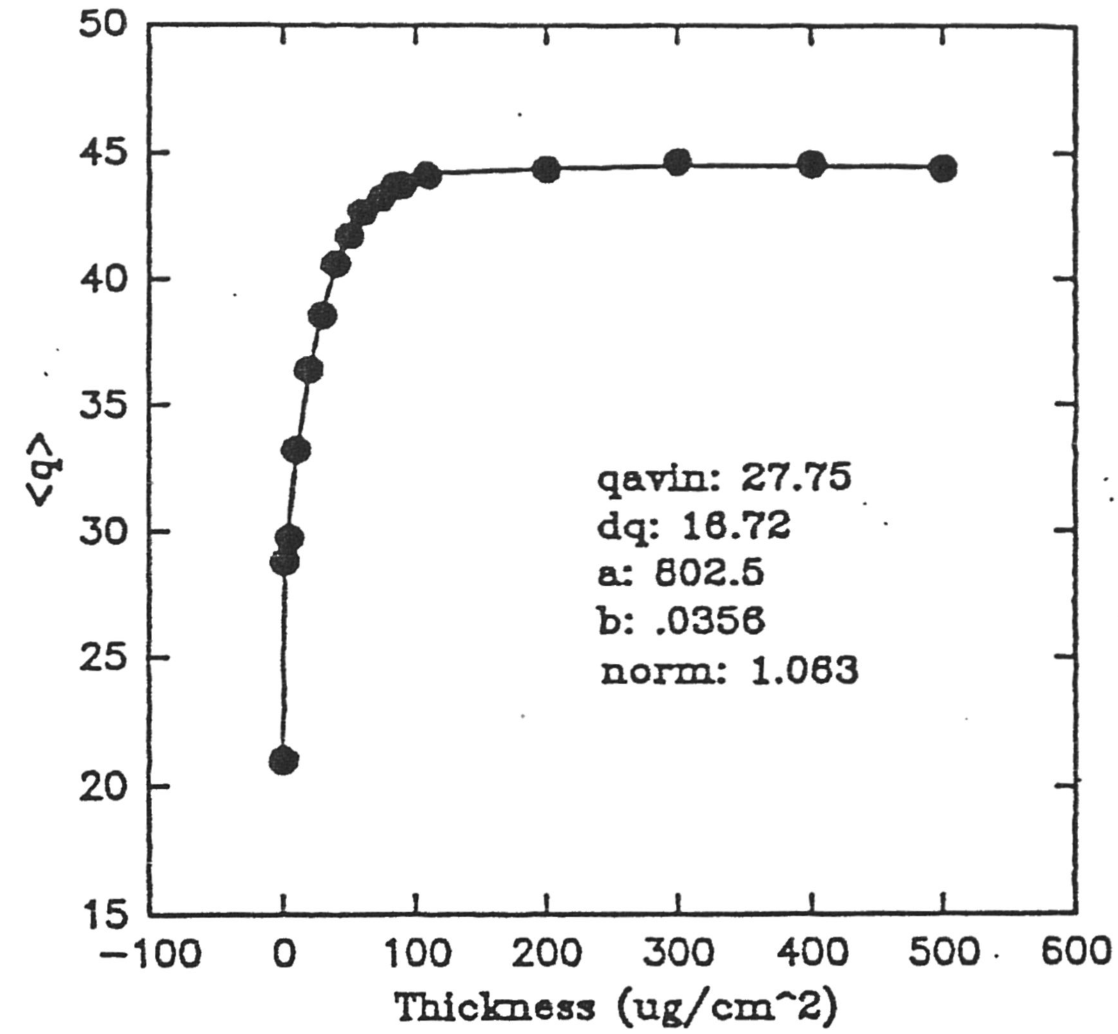

Figure 19. SigmaPlot fit of thickness dependence of average charge using model with only q_I fixed.

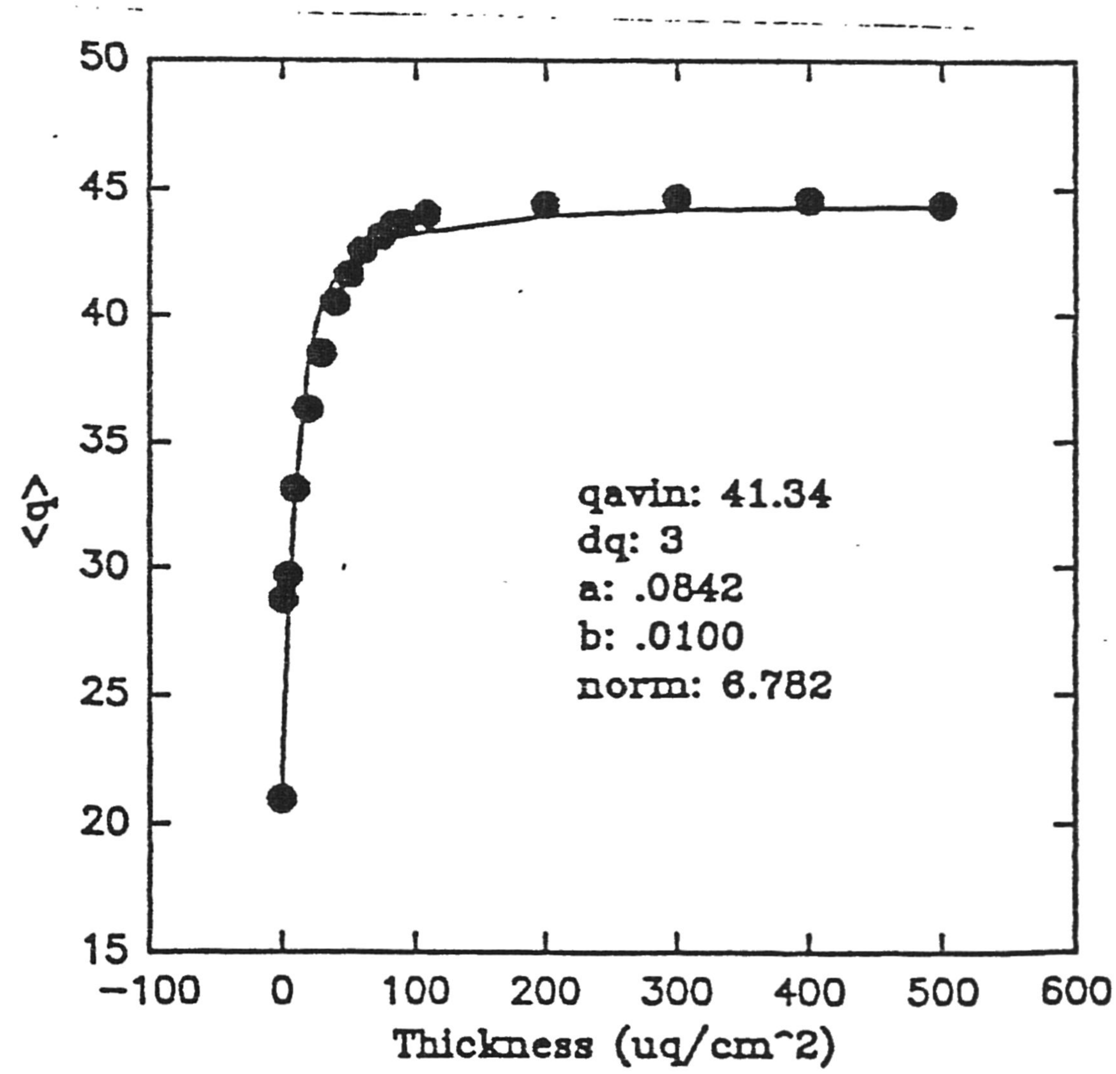

Figure 20. SigmaPlot fit of thickness dependence of average charge using model with both q_I and ΔQ fixed.

ΔQ=3 corresponds to the average charge change found by the x-ray experiments. Because the values of the constants a and b in this model are not the same, the model predicts that the thickness dependence of the inner shell vacancies in the ions is different from the thickness dependence of the average charge.

B. Double Foils

The model developed to describe the thickness dependence of the average charge can be applied to the double foils. The determination of the predicted average charge is made applying the formula, with the parameters determined by the fit of the single foil curve, to the upstream foil with $q_I=21^+$ and then applying the formula to the downstream foil but setting $q_I=\langle q\rangle_o$ from the first calculation. The model was applied to the double foils using the parameters from the first fit, with ΔQ=16.72, and from the second fit, with ΔQ=3. When the parameters from the first fit are used, no difference is predicted between the resulting average charges for the two orientations because the term containing q_I is negligible. When the parameters determined by the second, more physically realistic, fit is used, the discrepancy between the two orientations of the foils is reproduced. The predicted average charges are as shown in Table 1, where the upstream foil is listed first:

	Model	**Experimental**
30+74 μg/cm^2	42.91	44.06
74+30 μg/cm^2	42.24	43.52
60+90 μg/cm^2	43.12	44.63
90+60 μg/cm^2	42.71	44.36
50+200 μg/cm^2	43.93	45.63
200+50 μg/cm^2	42.56	44.84

Table 1. Predicted and measured average charges for the double foil targets.

These results show that, although the predicted average charge state deviated from the experimentally determined average charge states, the model does reproduce the relative magnitude of the discrepancies between the average charge states of the two orientations quite well.

VI. Conclusions

Five main conclusions can be drawn from this work:

(1) The equilibrium average charge and charge distribution that results from 8 MeV/μ Xe^{21+} impinging on carbon foils is predicted well by existing semi-empirical formulas, indicating that the validity of these formulas does hold at higher energies with heavier projectiles.

(2) An effect is present that causes the charge distributions of double foils to be dependent on the orientation of the foil.

(3) This double foil effect is related to Auger decays occurring after the beam exits the foil.

(4) The inner shell vacancies in the projectile are thickness dependent, and furthermore the thickness dependence of these inner shell vacancies is different from the thickness dependence of the average charge.

(5) The proposed model predicts the double foil effect.

The orientation dependence of double foil charge distributions is an unexpected and interesting discovery, and more research should be undertaken in order to better quantify the effect.

References

1. A.B. Wittkower and H.D. Betz. *Atomic Data* 5(2) (1973), 114.

2. K. Shima, T. Ishihora, T. Miyoshi, and T. Mikumo. *Phys. Rev.* A28 (1983), 2162.

3. A. Brunelle, S. Della-Negra, J. DePauw, H. Joret, Y. LeBeyec, and K. Wien. *Nucl. Instr. and Meth.* B43 (1989), 484.

4. J.A. Martin, R.L. Auble, K.A. Erb, C.M. Jones, and D.K. Olsen. *Nucl. Instr. and Meth.* A244 (1986), 187.

5. E. Baron and B. Delaunay. *Phys. Rev.* A12 (1975), 40.

6. R.D. Sayer, *Rev. Physique Appl.* 12 (1977), 1543.

7. V.S. Nikolaev and I.S. Dimitriev. *Phys. Lett.* 28A (1968), 277.

8. K. Shima, T. Ishihara, and T. Mikumo. *Nucl. Instr. and Meth.* 200 (1982), 605.

9. H.D. Betz and L. Grodzins. *Phys. Rev. Lett.* 25 (1970), 211.

10. J. Kuo, S. McDonald, and E. Fox. *Sigma Plot 5.0 User's Manual*, Jandel Scientific (1986).